

# A Simple Electrode-Level Chemical Presodiation Route by Solution Spraying to Improve the Energy Density of Sodium-Ion Batteries

Xiaoxiao Liu, Yuchen Tan, Tongchao Liu, Wenyu Wang, Chunhao Li, Jun Lu,\* and Yongming Sun\*

The formation of a solid electrolyte interface (SEI) on the surface of a carbon anode consumes the active sodium ions from the cathode and reduces the energy density of sodium-ion batteries (SIBs). Herein, a simple electrode-level presodiation strategy by spraying a sodium naphthalene (Naph-Na) solution onto a carbon electrode is reported, which compensates the initial sodium loss and improves the energy density of SIBs. After presodiation, an SEI layer is preformed on the surface of carbon anode before battery cycling. It is shown that a large irreversible capacity of  $60 \text{ mAh g}^{-1}$  is replenished and 20% increase of the first-cycle Coulombic efficiency is achieved for a hard carbon anode using this presodiation strategy, and the energy density of a  $\text{Na}_{0.9}[\text{Cu}_{0.22}\text{Fe}_{0.30}\text{Mn}_{0.48}]\text{O}_2$ |carbon full cell is increased from 141 to  $240 \text{ Wh kg}^{-1}$  by using the presodiated carbon anode. This simple and scalable electrode-level chemical presodiation route also shows generality and value for the presodiation of other anodes in SIBs.

stability, and notable corrosion resistance etc.<sup>[6–10]</sup> However, one serious problem for carbon anodes is their low initial Coulombic efficiency (usually less than 80%), which primarily originates from the irreversible sodium trapping and the formation of a solid electrolyte interphase (SEI) layer on the carbon surface during the initial sodiation process.<sup>[11,12]</sup> In other words, appreciable electrochemical active sodium ions from the cathode are consumed in the first charging process in a full battery with a carbon anode, which reduces the overall energy density of SIBs. Till now, successful examples have been shown to compensate the initial lithium loss in lithium-ion batteries (LIBs) by utilizing excess lithium sources through prelithiation.<sup>[13–15]</sup> Borrowed the idea from LIBs, presodiation will play an important

role in addressing the problem of the initial sodium loss and improving the electrochemical performances of SIBs.

Several presodiation techniques have been developed so far to offset the initial sodium loss in SIBs. Sodium-enriched positive electrodes were used to provide excess capacities during the battery charging process and increased energy density was achieved for the full cells using the as-prepared sodium-rich positive electrodes.<sup>[16]</sup> An electrochemical route was explored for the presodiation of a hard carbon anode in a half cell configuration using sodium metal as the counter electrode. A  $\text{NaNi}_{0.5}\text{Mn}_{0.5}\text{O}_2$ |carbon full cell with a presodiated hard carbon anode showed higher reversible capacities than the counterpart with a pristine hard carbon anode.<sup>[17]</sup> However, electrochemical presodiation procedure is time-consuming and complicated, and thus not suitable for industrial application. Another presodiation approach was using sacrificial sodium sources, including  $\text{NaN}_3$ ,<sup>[18,19]</sup>  $\text{Na}_2\text{C}_4\text{O}_4$ ,<sup>[20]</sup> and sodium metal powders,<sup>[21]</sup> as the presodiation additives for the electrodes. Nevertheless, undesired  $\text{N}_2$  or  $\text{CO}_2$  gas would generate during the electrochemical decomposition process of  $\text{NaN}_3$  or  $\text{Na}_2\text{C}_4\text{O}_4$ . The using of sodium metal powder might cause safety concerns due to the high chemical reactivity and instability, making it challenging for scale-up application. Thus, it remains highly desirable but challenging to explore a simple and high-efficiency presodiation approach in consideration of the practical application in battery industry.


## 1. Introduction

Sodium-ion battery (SIB) is one of the promising choices for grid-scale energy storage systems owing to the abundant reserves of sodium element in the crust and its low cost.<sup>[1–5]</sup> Carbon-based materials are considered to be one of the most promising anodes in SIBs for industrialization in the near term benefiting from their excellent conductivity, good structural

Dr. X. Liu, Y. Tan, W. Wang, C. Li, Prof. Y. Sun  
Wuhan National Laboratory for Optoelectronics  
Huazhong University of Science and Technology  
Wuhan 430074, China  
E-mail: yongmingsun@hust.edu.cn

T. Liu, Prof. J. Lu  
Chemical Sciences and Engineering Division  
Argonne National Laboratory  
Lemont, IL 60439, USA  
E-mail: junlu@anl.gov

T. Liu  
School of Advanced Materials  
Peking University  
Shenzhen Graduate School  
Shenzhen 518055, China

 The ORCID identification number(s) for the author(s) of this article can be found under <https://doi.org/10.1002/adfm.201903795>.

DOI: 10.1002/adfm.201903795

In this work, we develop a simple and novel electrode-level presodiation route that not only preforms a SEI layer on the hard carbon anode surface, but also prestores certain amount of active sodium ions into the carbon anode effectively without producing undesired side products or introducing any inert residues into the electrode. The presodiation process is conducted by spraying a designed presodiation solution, sodium naphthalene in tetrahydrofuran (THF), onto a hard carbon electrode with a subsequent drying process before battery assembly. In this process, the presodiation degree of the anode can be well controlled through adjusting the dosage of the presodiation solution. Moreover, such a presodiation process is performed at the electrode level without destroying the original structure of the electrode or material. As an example, a hard carbon anode with presodiation exhibited much higher initial Coulombic efficiency than the counterpart without presodiation (87% vs 67%) and an irreversible specific capacity of 60 mAh g<sup>-1</sup> was compensated by this presodiation approach. Furthermore, we demonstrated that a Na<sub>0.9</sub>[Cu<sub>0.22</sub>Fe<sub>0.30</sub>Mn<sub>0.48</sub>]O<sub>2</sub>||carbon full cell with a presodiated carbon anode showed dramatically increase in capacity and energy density in comparison to the Na<sub>0.9</sub>[Cu<sub>0.22</sub>Fe<sub>0.30</sub>Mn<sub>0.48</sub>]O<sub>2</sub>||carbon full cell with a pristine carbon anode. Moreover, this simple presodiation approach can also be applied to other anodes for SIBs (e.g., TiO<sub>2</sub> and Sn) and also shows generality to LIBs.

## 2. Results and Discussion

The presodiation process is illustrated in **Figure 1a**. Commercial naphthalene crystals were first dissolved in tetrahydrofuran. Sodium metal was then added with a Na/naphthalene molar ratio of 1/1. After the reaction between naphthalene and sodium metal in THF, 0.1 M sodium naphthalene (Naph-Na)

solution was finally obtained. The presodiation of the hard carbon electrode was realized by spraying the as-prepared Naph-Na solution onto the electrode for the presodiation reaction followed by a drying process to remove the solvent (THF) and the side product (naphthalene). It is noted that the THF solvent and naphthalene are not consumed in this presodiation process and can be recycled in future industrial applications, which can reduce the cost and avoid the environmental pollution. Benefiting from the liquid phase of the novel presodiation reagent, the presodiation process is simple and controllable. As shown in **Figure 1b**, due to its low redox potential and strong reducibility, Naph-Na can react with oxygen-containing functional groups on hard carbon anodes to generate Na-containing functional groups and a SEI layer can be formed on the surface of the presodiated carbon electrode when it is immersed into liquid electrolytes.<sup>[22,23]</sup> In a sodium-ion full battery, certain amount of sodium ions from the cathode are consumed to form a SEI layer on the carbon anode surface during the initial battery charging process and the remaining active sodium ions intercalate into the carbon anode, contributing the reversible capacity of the full batteries (**Figure S1a**, Supporting Information). In our experiment, by the preformation of a SEI layer on the anode surface before cycling, the consumption of electrochemical active sodium ions from cathodes can be reduced, and the energy density of SIBs can be increased (**Figure S1b**, Supporting Information). Note that the appropriate presodiation degree of the hard carbon anode is critical for capacity matching of positive and negative electrodes in a full cell. Insufficient sodiation donation would not fully address the irreversible sodium loss, while oversodiation might lead to the formation of sodium metal dendrites during battery cycling and cause safety concerns. Thus, an ideal degree of presodiation should fully offset the sodium loss in the initial cycle and meanwhile avoid introducing excess sodium ions.

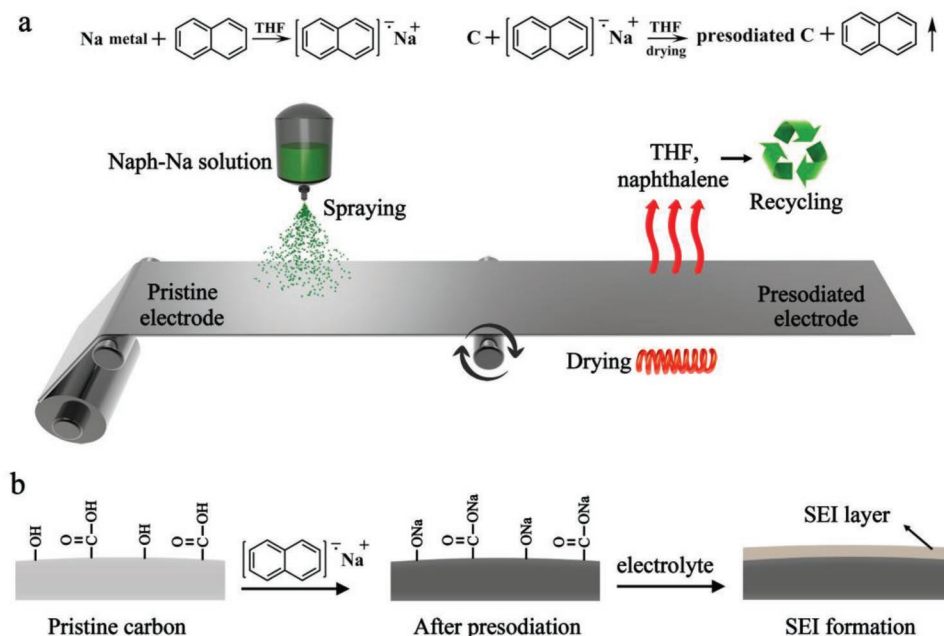


**Figure 1.** a) Schematic of the presodiation process at the electrode level and b) the presodiation mechanism of hard carbon electrodes using a Naph-Na solution as the presodiation reagent.

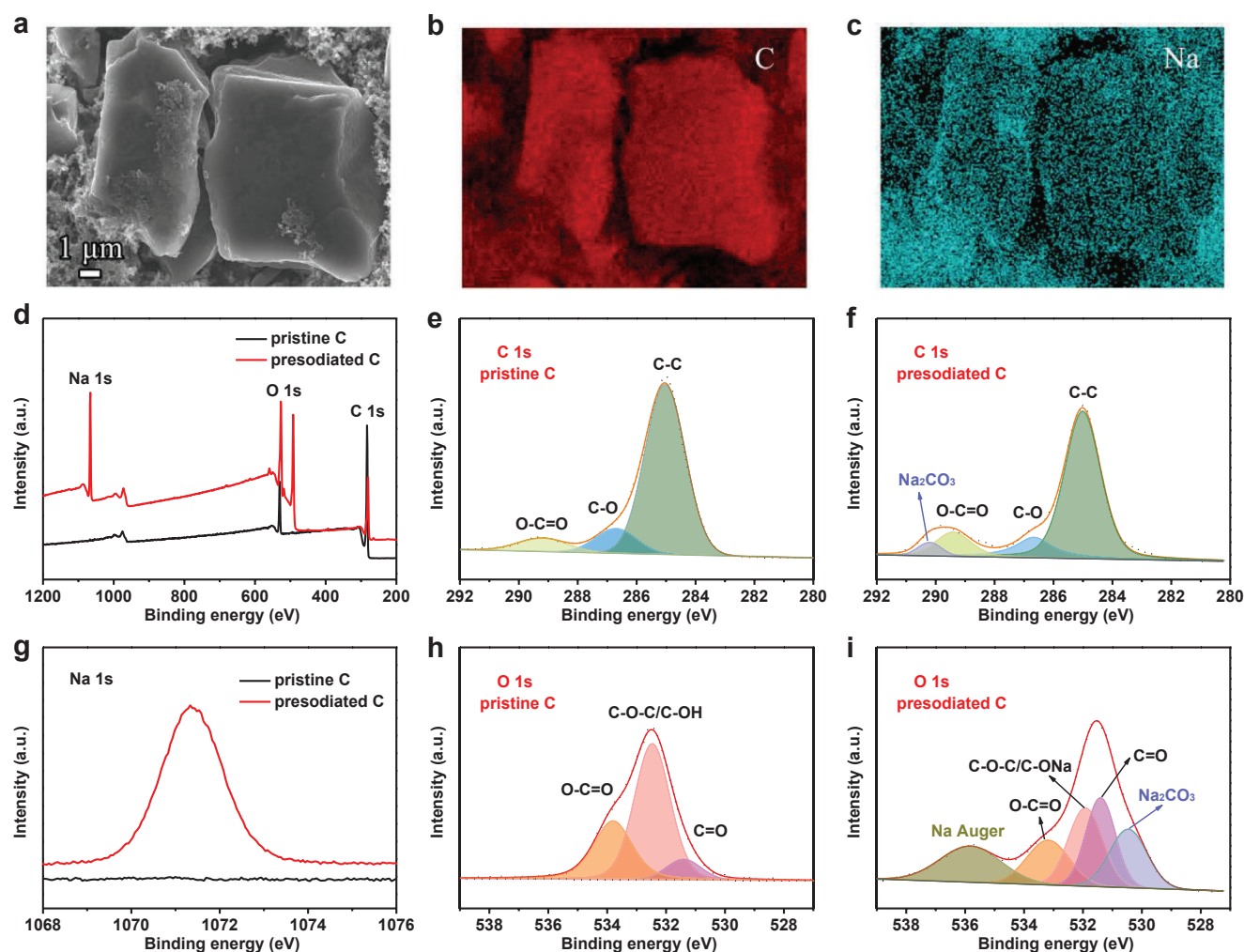


**Figure 2.** a) SEM image of the presodiated carbon electrode and the corresponding elemental mapping images of b) C and c) Na. d) Survey XPS spectra and high-resolution e,f) C 1s, g) Na 1s and h,i) O 1s XPS spectra of the pristine carbon and presodiated carbon.

Residuals in the electrode after presodiation cause the decrease of the overall energy density of batteries and may have negative effects on the cycling performance of batteries. Thus, an ideal presodiation approach should not introduce any residuals into the electrode. The results of Raman spectra showed that no signal of naphthalene was detected on the presodiated carbon electrode, indicating that the naphthalene side product of the presodiation reaction was completely removed after the drying process (Figure S2, Supporting Information). Therefore, only sodium is introduced into the carbon electrode using our presodiation approach, which is favorable for maximizing the overall energy density of a battery. Besides, the presodiation process has negligible influence on the Brunauer–Emmett–Teller (BET) surface area of the hard carbon (Figure S3, Supporting Information). The simple and low-cost process makes such a presodiation approach promising for practical applications.

Scanning electron microscope (SEM) and X-ray photoelectron spectroscopy (XPS) were conducted to investigate the morphology and surface structure of the carbon electrodes before and after presodiation. As displayed in Figures S4 and S5 (Supporting Information), the overall morphology and structure

of the carbon electrode remained unchanged after presodiation. The elemental mapping analysis revealed the uniform distribution of sodium element over the whole carbon electrode after presodiation, suggesting the uniform presodiation reaction (Figure 2a–c). XPS results indicated that the commercialized carbon material contained a certain amount of oxygen functional groups (Figure 2d,e,h). These functional groups could react with active sodium ions from the cathode during the first-cycle charging process, leading to a loss of active sodium ions and a decrease of the energy density of SIBs. After presodiation, a strong Na 1s peak at 1071.4 eV was produced (Figure 2d,g). Meanwhile, new peaks at 290.2 and 530.5 eV appeared for the presodiated carbon (Figure 2f,i), which could be ascribed to Na<sub>2</sub>CO<sub>3</sub>.<sup>[12,24]</sup> In comparison with the pristine hard carbon, the presodiated hard carbon shows a stronger broad peak at  $\approx$ 531.3 eV in the O 1s spectrum, which can be ascribed to the characteristic of sodium alkyl carbonate and sodium carboxylate.<sup>[12]</sup> According to the elemental analysis and high-resolution XPS spectra of C 1s and O 1s, the –OH and –COOH functional groups in hard carbon converted to –ONa and –COONa after presodiation. These results indicated that the nature of surface

chemistry of the carbon was changed after presodiation. With a combination of the SEM and XPS results, it is inferred that our presodiation strategy using a Naph-Na solution as the presodiation reagent is successful in the presodiation of hard carbon electrodes, and thus the first-cycle Coulombic efficiency and energy density of SIBs can be improved.

High presodiation efficiency and good stability of the presodiated electrode are both important criterions for the practical application of presodiation techniques in industry. The electrochemical behaviors of the carbon electrodes with and without presodiation were investigated using cyclic voltammetry (CV) and galvanostatic charge/discharge measurements in both half cells and full cells. The sodium-ion storage property of the carbon electrodes with and without presodiation was first evaluated in the potential range of 0.01–1.5 V at the current density of 0.1 C (1 C = 250 mA g<sup>-1</sup>) in a half cell configuration using sodium metal as the counter electrode. As shown in Figure 3a, the first-cycle sodiation profiles of the carbon

electrode with and without presodiation exhibited a remarkable difference. The open circuit voltage (OCV) decreased from 2.35 V for the carbon electrode without presodiation to 0.75 V for the electrode with presodiation, suggesting that sodium was prestored into the carbon electrode due to the low redox potential of Naph-Na. Compared with the pristine carbon electrode, the irreversible voltage slope between 0.7 and 1.2 V disappeared for the presodiated carbon electrode during the initial electrochemical sodiation process (Figure 3a), indicating that this irreversible reaction was mitigated by presodiation. This result, together with the XPS results, indicated that a SEI layer was preformed on the presodiated carbon surface before battery cycling, which reduced the consumption of the electrolyte and active sodium ions from the cathode side.<sup>[25,26]</sup> Benefiting from the alleviation of the irreversible sodium loss, a high specific capacity of 60 mAh g<sup>-1</sup> was effectively compensated, resulting in an increase of initial Coulombic efficiency from 67% to 87%. It should be noted that the presodiation degree of the anode

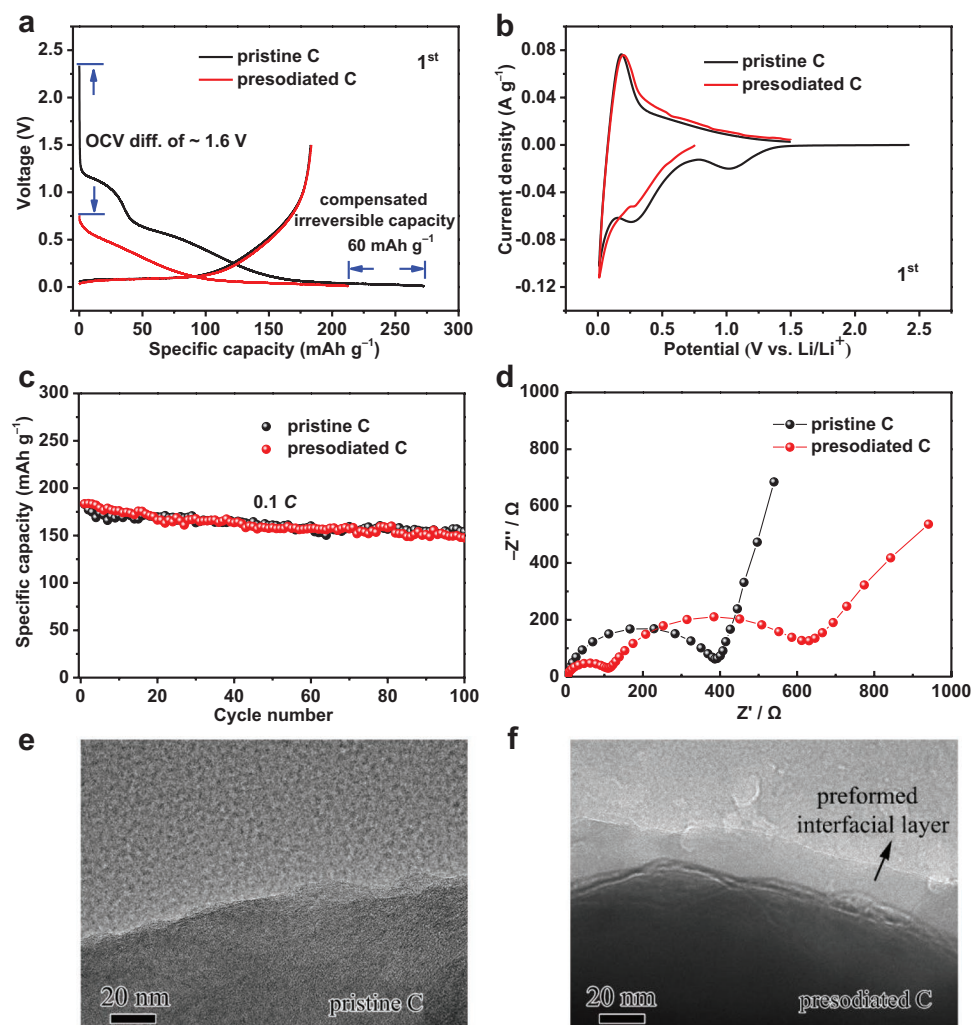


**Figure 3.** Electrochemical performances of the carbon electrodes with and without presodiation. a) The voltage-capacity curves of the pristine and presodiated carbon electrode for the first charge/discharge cycle. b) CVs of the pristine and presodiated carbon electrode for the first charge/discharge cycle. c) Cycling stability and d) EIS study of the pristine and presodiated carbon electrode. TEM images of e) the pristine and f) presodiated carbon after immersed in a liquid electrolyte before battery cycling.



can be well turned through adjusting the dosages of the presodiation solution. Using different dosages of a 0.1 M Naph-Na/THF solution, carbon electrodes with different presodiation degrees were achieved (Figure S6, Supporting Information). Therefore, our presodiation method here is capable of reducing the decomposition of liquid electrolyte, compensating partial sodium loss, and increasing the initial Coulombic efficiency of SIBs.

The first-cycle desodiation capacities of the hard carbon anodes with and without presodiation were similar (Figure 3a) and their second-cycle voltage-capacity plots overlapped well (Figure S7a, Supporting Information), suggesting that the presodiation had no negative effects on the desodiation property of the hard carbon electrodes. The CVs of the pristine and presodiated carbon electrodes for the initial two cycles were compared in Figure 3b and Figure S7b (Supporting Information). The pristine carbon electrode exhibited a broad reduction peak in the potential range of 0.75–1.3 V, which could be assigned to the irreversible reactions between the electrode and electrolyte, and the formation of SEI.<sup>[27,28]</sup> In contrast, this reduction peak disappeared for the presodiated hard carbon electrode, well consistent with their first-cycle sodiation profiles (Figure 3b). The second-cycle CV profiles of the electrodes with and without presodiation overlapped well, indicating that the presodiation did not have any negative effects on the sodiation/desodiation properties after the first cycle (Figure S7b, Supporting Information). To further investigate the effect of presodiation on the long-term electrochemical stability of the carbon electrodes, we evaluated the cycling performances of the two samples under galvanostatic mode. As shown in Figure 3c, good cycling stability was achieved for the hard carbon electrodes with and without presodiation for 100 cycles in a half cell configuration using sodium metal as the counter electrode. Therefore, not only the presodiation of hard carbon electrode supplies appropriate sodium ions to offset the initial sodium loss, but also good structural stability and electrochemical performances of the hard carbon electrode are maintained after presodiation.

The electrochemical impedance spectroscopy (EIS), transmission electron microscopy (TEM), attenuated total reflectance-Fourier transform infrared (ATR-FTIR) spectrum, and XPS were performed to investigate the presodiated carbon electrode for better understanding its improved electrochemical performance. The EIS spectra of the pristine and presodiated carbon electrodes before cycling were shown in Figure 3d. A new semicircle at high frequency region emerged for the presodiated carbon electrode, suggesting the preformation of an interfacial layer on the carbon electrode surface, corresponding well with the first-cycle charge/discharge curves and CV results (Figure 3a,b). This result was also confirmed by TEM, XPS, and ATR-FTIR investigations. In comparison with the clear surface of the bare carbon, an interfacial layer with a thickness of  $\approx 20$  nm was observed for the presodiated carbon (Figure 3e,f). The XPS and ATR-FTIR results indicated that this interfacial layer, the preformed SEI layer, consisted of some sodium containing-organic and inorganic compounds, such as sodium alkyl carbonates, sodium carboxylate,  $\text{Na}_2\text{CO}_3$ , NaF, etc. (Figure S8, Supporting Information).<sup>[12,26,29]</sup> Besides, according to the desodiation curves of the carbon electrodes before cycling (Figure S9, Supporting Information), a certain amount of sodium-ion capacity was

achieved during the desodiation process of the presodiated electrode, indicating the successful introduction of active sodium ions into the carbon electrode by presodiation. Therefore, the proposed novel presodiation route not only preforms a SEI layer on the surface of the hard carbon before electrochemical cycling, but also prestores certain amount of electrochemically active sodium ions into the hard carbon anode. This preformed interfacial layer, the so called preformed SEI here, may be different from the normal SEI layer formed during electrochemical cycling, as both the salt and the solvents are different for the presodiation solution and electrolyte, also this preformed interfacial layer is chemically formed while the normal SEI is electrochemically formed. During the initial sodiation, the preformed interfacial layer may reconstruct under electrochemical condition, forming similar SEI to the pristine carbon. That is why the hard carbon electrodes with and without presodiation showed similar Nyquist plots (Figure S10, Supporting Information). The similar Nyquist plots of the hard carbon electrode with and without presodiation after cycling indicate that there is no negative influence for the hard carbon electrode with presodiation.

To show the important role of presodiation in improving the energy density of full batteries, full cells using  $\text{Na}_{0.9}[\text{Cu}_{0.22}\text{Fe}_{0.30}\text{Mn}_{0.48}]\text{O}_2$  as the cathode and hard carbon as the anode were constructed (Figure 4a). Figure 4b showed the voltage-capacity profiles of the  $\text{Na}_{0.9}[\text{Cu}_{0.22}\text{Fe}_{0.30}\text{Mn}_{0.48}]\text{O}_2$ /carbon cells with and without anode presodiation in the potential range of 1–4 V at 0.1 C (1 C = 150 mA g<sup>-1</sup>) for the first cycle. In the initial charge process, both full cells exhibited a similar charge capacity of around 156 mAh g<sup>-1</sup>. However, they showed very different discharge capacities. The full cell with a presodiated carbon anode delivered a high initial discharge capacity of 145 mAh g<sup>-1</sup>. In a sharp contrast, the discharge specific capacities of the full cell with a pristine carbon anode was only 83 and 62 mAh g<sup>-1</sup> lower than that of the full cell with a presodiated carbon anode. The increased discharge capacity of the full cell with the presodiated carbon electrode came from the compensated sodium ions by the presodiation. Moreover, the full cell with a presodiated carbon anode maintained a much higher capacity than the full cell with a pristine carbon anode over cycling. After 20 cycles, the presodiated full cell still delivered a high specific capacity of 127 and 62 mAh g<sup>-1</sup> higher than the full cell with a pristine carbon anode (Figure 4c). This result suggests that our presodiation approach can improve the overall energy density of SIBs as well as maintaining good cycling stability. Since only the active sodium is donated into the carbon anode without any other inert residues, the overall energy density based on both the anode and cathode is maximized. The energy density of the fabricated 3.0 V class full cell with a presodiated carbon anode is about 240 Wh kg<sup>-1</sup>, which is much higher than 141 Wh kg<sup>-1</sup> for the full cell with a pristine carbon anode.

To show the generality of this presodiation approach, we also have presodiated  $\text{TiO}_2$  and Sn electrodes using Naph-Na/THF solution as the presodiation reagent with the same procedure.  $\text{TiO}_2$  and Sn powders were used to show the color change before and after presodiation. After presodiation, the color of  $\text{TiO}_2$  powders changed from white to dark green (Figure 5a,b) and the Sn powders turned to dark gray from light

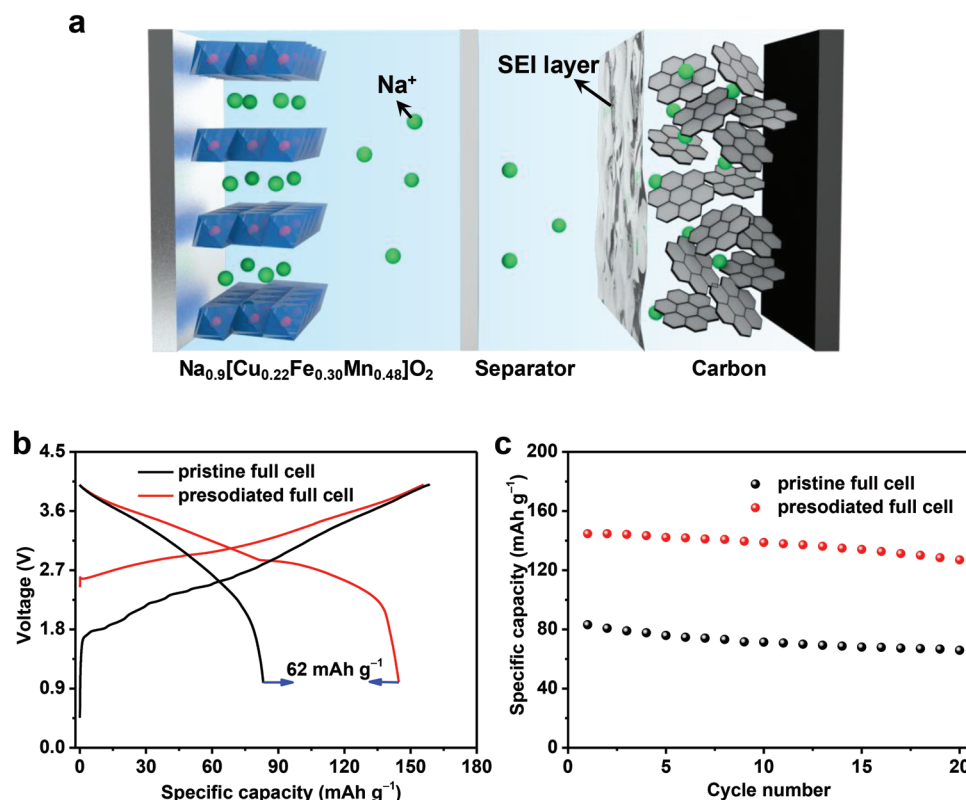


**Figure 4.** a) Schematic illustration of a sodium-ion full cell using a  $\text{Na}_{0.9}[\text{Cu}_{0.22}\text{Fe}_{0.30}\text{Mn}_{0.48}]\text{O}_2$  cathode and a carbon anode with a preformed SEI. b) The first-cycle charge/discharge curves and c) cycling performance of sodium-ion full cells with a pristine and a presodiated carbon anode, respectively.

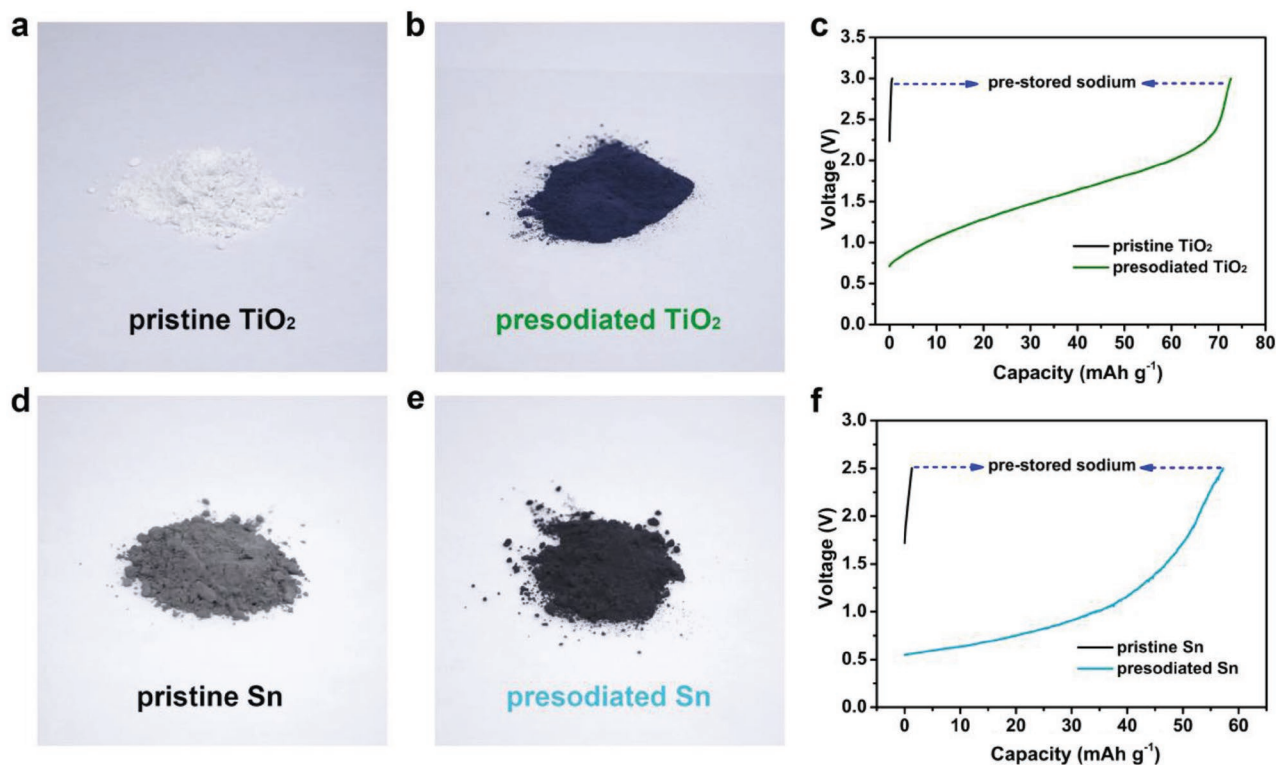


**Figure 5.** Photographs of the pristine and presodiated a,b)  $\text{TiO}_2$  and d,e) Sn powders. The de-sodiation process of the pristine and presodiated c)  $\text{TiO}_2$  and f) Sn electrodes before cycling. The current density for the de-sodiation process is  $20 \text{ mA g}^{-1}$ .

gray (Figure 5d,e), indicating the reaction between both powders with Naph-Na solution. The  $\text{TiO}_2$  remained a rutile phase, while the Sn converted into Na-Sn alloys after presodiation (Figure S11, Supporting Information). Similar to the presodiated carbon electrode, both presodiated  $\text{TiO}_2$  and Sn electrodes possessed lower OCV than their pristine counterparts (Figure 5c,f). The presodiated  $\text{TiO}_2$  and Sn electrodes delivered a high specific charge capacity of 72 and 57  $\text{mAh g}^{-1}$  before cycling, respectively, suggesting their successful presodiation. In addition, we also showed that this presodiation approach could be easily generalized to the prelithiation of carbon anode for LIBs and improve the initial Coulombic efficiency (Figure S12, Supporting Information).

### 3. Conclusion

In conclusion, the present work demonstrated a simple and high-efficiency electrode-level presodiation approach to compensate the initial sodium loss and improve the energy density of SIBs. The presodiation process is conducted in a facile and controllable way by spraying a Naph-Na solution onto a hard carbon electrode followed by a drying process, and is potentially feasible for the industrial application. The presented presodiation approach does not introduce any inert residues into the electrode, and therefore can maximize presodiation efficiency and energy density of the full batteries. In a half cell configuration using a sodium metal counter electrode, remarkable improvement in the initial Coulombic efficiency and efficient mitigation of irreversible capacity were achieved for a carbon electrode with presodiation. In a full cell configuration with a  $\text{Na}_{0.9}[\text{Cu}_{0.22}\text{Fe}_{0.30}\text{Mn}_{0.48}]\text{O}_2$  cathode and a hard carbon anode with presodiation, much improved capacity and energy density were realized. Moreover, this simple presodiation approach was generalized to other anode materials for SIBs with large first-cycle irreversible capacity loss, such as metal oxides-based and alloy-based anodes (e.g.,  $\text{TiO}_2$  and Sn). Therefore, we believe that this facile and high-efficiency presodiation approach will advance the development of SIBs with higher energy density.

### 3. Experimental Section

**Materials Preparation:** Commercialized hard carbon materials,  $\text{TiO}_2$  and Sn powders were used as received without any further treatment.  $\text{Na}_{0.9}[\text{Cu}_{0.22}\text{Fe}_{0.30}\text{Mn}_{0.48}]\text{O}_2$  particles were prepared using a solid state reaction method referring to the previous literature.<sup>[30]</sup> 4.77 g  $\text{Na}_2\text{CO}_3$ , 1.75 g CuO, 2.40 g  $\text{Fe}_2\text{O}_3$ , and 3.79 g  $\text{Mn}_2\text{O}_3$  were ball-milled at 350  $\text{rpm s}^{-1}$  on the planetary ball mill equipment (MITR) for 6 h. After homogeneously mixing the precursor, the obtained powders were heated in air at 850  $^{\circ}\text{C}$  for 15 h. The morphology, phase and electrochemical characterizations of  $\text{Na}_{0.9}[\text{Cu}_{0.22}\text{Fe}_{0.30}\text{Mn}_{0.48}]\text{O}_2$  particles were shown in Figure S13 (Supporting Information). 0.1 M sodium naphthalene (Naph-Na) solution was prepared by dissolving the naphthalene crystals and sodium metal into tetrahydrofuran. The presodiation process was performed by spraying the as-prepared Naph-Na solution onto the hard carbon electrode with the dosage of 38  $\mu\text{L cm}^{-2}$  followed by drying. The dosage of the Naph-Na solution for presodiation was calculated based on the theoretical value to realize 100% initial Coulombic efficiency for the hard carbon electrode. For the preparation of presodiated  $\text{TiO}_2$  and Sn powders, pristine powders were immersed into excess amount

of 1 M Naph-Na solutions for 0.5 h, then the as-obtained powders were collected after washing with THF for three times. The procedure for presodiation of  $\text{TiO}_2$  and Sn electrodes is similar to that of hard carbon electrodes.

**Materials Characterization:** The morphology of the electrodes and materials was characterized by scanning electron microscopy equipped with an energy spectrometer (Nova NanoSEM 450). Raman spectroscopy was collected on a confocal Raman spectrometer (LabRAM HR800, Horiba JobinYvon) using a 532 nm excitation laser. X-ray diffraction (XRD) patterns were collected on a PANalytical B.V. instrument (Empyrean) with  $\text{Cu-K}\alpha 1$  radiation operated at an accelerating voltage of 40 kV and current of 40 mA. X-ray photoelectron spectroscopy was performed on a VG MultiLab 2000 system (Thermo VG Scientific) using a monochromatic Al  $\text{K}\alpha$  X-ray source. Nitrogen adsorption/desorption isotherms were detected using an ASAP 2460 apparatus (Micromeritics). Attenuated total reflectance-Fourier transform infrared spectra were collected by applying the VERTEX 70 (Bruker) spectrometer.

**Electrochemical Characterization:** Slurry for hard carbon,  $\text{TiO}_2$ , and Sn negative electrodes were prepared by mixing 80 wt% commercial active material, 10 wt% carbon black, and 10 wt% poly(vinylidene fluoride) binder (PVDF) in *N*-methyl-2-pyrrolidinone. The slurry was then casted onto a copper foil current collector using a doctor blade and dried at 80  $^{\circ}\text{C}$  for 6 h to fabricate the negative electrode. The mass loading of hard carbon active material was  $\approx 1.2 \text{ mg cm}^{-2}$ . The fabrication process of the positive electrode was similar to the negative electrode using the home-made  $\text{Na}_{0.9}[\text{Cu}_{0.22}\text{Fe}_{0.30}\text{Mn}_{0.48}]\text{O}_2$  powder as the active material and an Aluminum foil as the current collector. The capacity ratio of negative to positive electrode was 1.08 for the  $\text{Na}_{0.9}[\text{Cu}_{0.22}\text{Fe}_{0.30}\text{Mn}_{0.48}]\text{O}_2$ /carbon full cell. All cells were assembled using CR2032-type coin cells in an Argon-filled glove box with  $\text{H}_2\text{O} < 0.1 \text{ ppm}$  and  $\text{O}_2 < 0.1 \text{ ppm}$ . The separator was glass fibers (Whatman) and the electrolyte was 1 M  $\text{NaClO}_4$  in ethylene carbonate (EC) and dimethyl carbonate (DMC) with addition of 2 vol% fluoroethylene carbonate (FEC). The galvanostatic charge/discharge measurements of the cells were carried out on a multichannel battery testing instrument (Neware, China). The cyclic voltammetry and electrochemical impedance spectroscopy were recorded on a VMP3 multichannel potentiostat (Bio-Logic). Hard carbon electrodes were galvanostatically charged and discharged in the potential range of 0.01–1.5 V at 0.1 C (1 C = 250  $\text{mA g}^{-1}$ ) using sodium metal as the counter electrode in a half cell configuration.  $\text{Na}_{0.9}[\text{Cu}_{0.22}\text{Fe}_{0.30}\text{Mn}_{0.48}]\text{O}_2$ /Na metal half cells were evaluated in the potential range of 2.5–4.0 V at 0.1 C.  $\text{Na}_{0.9}[\text{Cu}_{0.22}\text{Fe}_{0.30}\text{Mn}_{0.48}]\text{O}_2$ /C full cells were measured at a low current density of 0.1 C (1 C = 150  $\text{mA g}^{-1}$ ) in the potential range of 1–4 V. The energy density of the full cells was calculated based on the total mass of the active cathode and anode materials.

### Supporting Information

Supporting Information is available from the Wiley Online Library or from the author.

### Acknowledgements

X.L. and Y.T. contributed equally to this work. This work was supported by the Natural Science Foundation of China (Grant No. 51802105) and China Postdoctoral Science Foundation (Grant No. 0106187114). This work is also partially supported by the U.S. Department of Energy (DOE), Office of Energy Efficiency and Renewable Energy, Vehicle Technologies Office (DE-AC02-06CH11357). Argonne National Laboratory is operated for DOE Office of Science by UChicago Argonne, LLC. The authors would like to thank the Analytical and Testing Center of Huazhong University of Science and Technology as well as the Center for Nanoscale Characterization & Devices of Wuhan National Laboratory for Optoelectronics (2019) for providing the facilities to conduct the characterization.

## Conflict of Interest

The authors declare no conflict of interest.

## Keywords

carbon anodes, electrode levels, presodiation, sodium-ion batteries, solution spraying

Received: May 13, 2019

Revised: September 17, 2019

Published online: October 8, 2019

- [1] B. Dunn, H. Kamath, J. M. Tarascon, *Science* **2011**, 334, 928.
- [2] N. Yabuuchi, K. Kubota, M. Dahbi, S. Komaba, *Chem. Rev.* **2014**, 114, 11636.
- [3] M. D. Slater, D. Kim, E. Lee, C. S. Johnson, *Adv. Funct. Mater.* **2013**, 23, 947.
- [4] X. J. Wei, X. P. Wang, X. Tan, Q. Y. An, L. Q. Mai, *Adv. Funct. Mater.* **2018**, 28, 1804458.
- [5] W. Luo, F. Shen, C. Bommier, H. L. Zhu, X. L. Ji, L. B. Hu, *Acc. Chem. Res.* **2016**, 49, 231.
- [6] L. Zhang, X. X. Liu, Y. H. Dou, B. W. Zhang, H. L. Yang, S. X. Dou, H. K. Liu, Y. H. Huang, X. L. Hu, *Angew. Chem., Int. Ed.* **2017**, 56, 13790.
- [7] X. X. Liu, T. Shu, L. Zhang, F. Y. Li, X. L. Hu, *Carbon* **2019**, 143, 240.
- [8] Z. L. Jian, S. Y. Hwang, Z. F. Li, A. S. Hernandez, X. F. Wang, Z. Y. Xing, D. Su, X. L. Ji, *Adv. Funct. Mater.* **2017**, 27, 1700324.
- [9] Z. Y. Peng, Y. J. Hu, J. J. Wang, S. J. Liu, C. X. Li, Q. L. Jiang, J. Lu, X. Q. Zeng, P. Peng, F. F. Li, *Adv. Energy Mater.* **2019**, 9, 1802928.
- [10] F. Shen, W. Luo, J. Q. Dai, Y. G. Yao, M. W. Zhu, E. Hitz, Y. F. Tang, Y. F. Chen, V. L. Sprenkle, X. L. Li, L. B. Hu, *Adv. Energy Mater.* **2016**, 6, 1600377.
- [11] X. Zhao, Y. Ding, Q. Xu, X. Yu, Y. Liu, H. Shen, *Adv. Energy Mater.* **2019**, 9, 1803648.
- [12] S. Komaba, W. Murata, T. Ishikawa, N. Yabuuchi, T. Ozeki, T. Nakayama, A. Ogata, K. Gotoh, K. Fujiwara, *Adv. Funct. Mater.* **2011**, 21, 3859.
- [13] Y. M. Sun, H. W. Lee, Z. W. Seh, N. Liu, J. Sun, Y. Z. Li, Y. Cui, *Nat. Energy* **2016**, 1, 15008.
- [14] J. Zhao, Z. D. Lu, N. Liu, H. W. Lee, M. T. McDowell, Y. Cui, *Nat. Commun.* **2014**, 5, 5088.
- [15] H. J. Kim, S. Choi, S. J. Lee, M. W. Seo, J. G. Lee, E. Deniz, Y. J. Lee, E. K. Kim, J. W. Choi, *Nano Lett.* **2016**, 16, 282.
- [16] B. Zhang, R. Dugas, G. Rousse, P. Rozier, A. M. Abakumov, J. M. Tarascon, *Nat. Commun.* **2016**, 7, 10308.
- [17] E. de la Llave, V. Borgel, K. J. Park, J. Y. Hwang, Y. K. Sun, P. Hartmann, F. F. Chesneau, D. Aurbach, *ACS Appl. Mater. Interfaces* **2016**, 8, 1867.
- [18] G. Singh, B. Acebedo, M. C. Cabanas, D. Shanmukaraj, M. Armand, T. Rojo, *Electrochem. Commun.* **2013**, 37, 61.
- [19] J. Martinez De Ilarduya, L. Otaegui, J. M. López del Amo, M. Armand, G. Singh, *J. Power Sources* **2017**, 337, 197.
- [20] D. Shanmukaraj, K. Kretschmer, T. Sahu, W. Bao, T. Rojo, G. X. Wang, M. Armand, *ChemSusChem* **2018**, 11, 3286.
- [21] J. L. Tang, D. K. Kye, V. G. Pol, *J. Power Sources* **2018**, 396, 476.
- [22] J. Zheng, H. Zhang, S. H. Dong, Y. P. Liu, C. T. Nai, H. S. Shin, H. Y. Jeong, B. Liu, K. P. Loh, *Nat. Commun.* **2014**, 5, 2995.
- [23] R. Rodriguez, K. E. Loeffler, S. S. Nathan, J. K. Sheavly, A. Dolocan, A. Heller, C. B. Mullins, *ACS Energy Lett.* **2017**, 2, 2051.
- [24] D. Luo, J. Xu, Q. B. Guo, L. Z. Fang, X. H. Zhu, Q. Y. Xia, H. Xia, *Adv. Funct. Mater.* **2018**, 28, 1805371.
- [25] J. Zhao, Z. D. Lu, H. T. Wang, W. Liu, H. W. Lee, K. Yan, D. Zhuo, D. C. Lin, N. Liu, Y. Cui, *J. Am. Chem. Soc.* **2015**, 137, 8372.
- [26] F. A. Soto, P. F. Yan, M. H. Engelhard, A. Marzouk, C. M. Wang, G. L. Xu, Z. H. Chen, K. Amine, J. Liu, V. L. Sprenkle, F. El-Mellouhi, P. B. Balbuena, X. L. Li, *Adv. Mater.* **2017**, 29, 1606860.
- [27] X. Y. Wang, L. Fan, D. C. Gong, J. Zhu, Q. F. Zhang, B. A. Lu, *Adv. Funct. Mater.* **2016**, 26, 1104.
- [28] M. Anji Reddy, M. Helen, A. Groß, M. Fichtner, H. Euchner, *ACS Energy Lett.* **2018**, 3, 2851.
- [29] M. Y. Nie, J. Demeaux, B. T. Young, D. R. Heskett, Y. J. Chen, A. Bose, J. C. Woicik, B. L. Lucht, *J. Electrochem. Soc.* **2015**, 162, A7008.
- [30] L. Q. Mu, S. Y. Xu, Y. M. Li, Y. S. Hu, H. Li, L. Q. Chen, X. J. Huang, *Adv. Mater.* **2015**, 27, 6928.